THE BERILL FAULT AND ITS RELATION
TO A DEEP SEATED GRAVITATIONAL SLOPE DEFORMATION (DSGSD)

Ingvar KRIEGER [*], Reginald L. HERMANNS [**], Markus SCHLEIER[***],
Freddy Xavier YUGSI MOLINA[**], Thierry OPPIKOFER[**], Jan Steinar RØNNING[**],
Trond EIKEN[****] & Joachim ROHN[***]

[*] University of Erlangen-Nuremberg - GeoZentrum Nordbayern - Erlangen, Germany Now Isofer AG - Knonau, Switzerland
[**] Geological Survey of Norway - Trondheim, Norway
[***] University of Erlangen-Nuremberg - GeoZentrum Nordbayern - Erlangen, Germany
[****] University of Oslo - Oslo, Norway

ABSTRACT

Within the Innfjorddalen valley (Møre og Romsdal, Norway) a 1.5 km long linear NNE-SSW striking feature, forming a 3-4 m high step in the topography, occurs on the SE facing slope of the Middagstinden mountain and was previously discussed as a Holocene reverse fault, called the "Berill fault". Our intense structural field mapping and a high resolution digital elevation model based on LiDAR data derived from airborne and terrestrial laser scanning indicate that the "Berill fault" is a normal fault that has the orientation of the collapse of the Caledonian orogen, that is today reactivated as a limiting structure of a Deep Seated Gravitational Slope Deformation (DSGSD). Differential Global Navigation Satellite System (dGNSS) surveys over the instability indicate velocities of the DSGSD of ca. 0.6 cm/yr. Three electric resistivity profiles on the valley floor attest that the fault is a structure with regional extend. Three trenches with a total length of 100 m parallel to the electric resistivity profiles although down to glacial deposits or the underlying bedrock do not indicate any Holocene activity of the fault. Hence reactivation of the fault by the DSGSD produces the linear feature oblique to the slope.

***Key words:** normal fault, rock slope instability, LiDAR, kinematic analyses, Western Norway*

INTRODUCTION

Several km-long linear features that build a ver-tical step in high mountain terrain have often been discussed to be either related to faulting or to deep seated gravitational slope deformation (THOMPSON *et alii*, 1996; HIPPOLYTE *et alii*, 2006; LI *et alii*, 2010). The slope of the investigation area shows a promi-nent 1.5 km long linear feature, that strikes NNE-SSW and therefore in a 30 degree angle with the SE facing slope. It forms a 3-4 m high step in the topog-raphy and was previously discussed as a Holocene reverse fault called the "Berill fault" (ANDA *et alii*, 2002). Only on the western side of the fault a mas-sive rock slope instability has developed. Here oc-cur slope parallel, up to 20 meter deep up-hill facing scarps (counter scarps) with active rock fall and shal-low translational sliding of single rock blocks and unconsolidated rock (e.g. shallow landslides). East of the lineament called the "Berill fault" no slope deformation is visible. Hence the fault seems to be a limiting factor for the slope instability.

In order to better understand the relation of the slope deformation with the proposed Holocene re-verse fault, an intensive structural analyses of the slope and electric resistivity profile measurements along the valley floor were implemented and the deformation was monitored over the past 5 years with differential Global Navigation Satellite System (dGNSS) surveys. The investigation area is located on the south-east exposed slope of the Middagstin-den mountain right above the Berrilvatnet lake in the Møre og Romsal county in West Norway (Fig. 1) and
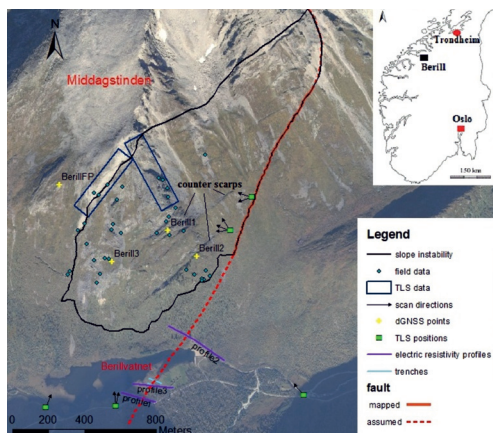
Fig. 1 - Orthophoto of the Berill instability (NGU) showing the different observation points for field data, TLS data and dGNSS measurements, the position of the trenches and the electric resistivity profiles and the morphological trace of the fault; The investigation is limited to the western part of the instability with rock outcrops, since the rest is covered by surficial glacial deposits that do not allow the implementation of structural analyses of the bedrock

herein it is described as the "Berill instability". The instable slope is part of the Innfjorddalen, a glacial U- valley, where several post glacial mass movements have taken place (SCHLEIER *et alii*, this issue).

GEOLOGICAL SETTING

The Berill instability is located in the Western Norwegian Gneiss Region (WNGR). The bedrock of this area consists mainly of proterozoic gneisses with a magmatic origin, which is locally covered with oceanic and continental sediments. The deformation and metamorphisation of the neo- and mesoproterozoic rocks took place during the Caledonian orogeny (GANERØD, 2008). In the geological map sheet the gneisses are described as undifferentiated and locally migmatitic in composition (TVETEN *et alii*, 1998). The most prevalent rock types in the WNGR are tonalitic and granodioritic gneisses (HACKER *et alii*, 2010). The bedrock disclosed in the investigation area is marked of quartz-dioritic gneiss with a sporadically well distinct foliation. Locally migmatitic structures are present (TVETEN *et alii*, 1998).

METHODS
DATA USED

A detailed structural field mapping over the whole investigation area with rock outcrops was undertaken and about 1500 structural measurements at 35 locations were taken. Furthermore the main features and the limiting structures in the instability were mapped in order to estimate the size of the individual blocks (Fig. 1 and 2).

Supplementary data for structural analyses was gained from airborne- and ground based LiDAR- (Light Detection and Ranging) data in order to create a high resolution digital elevation model (DEM). To create a DEM by terrestrial laser scanning (TLS) the site was scanned with the long range ILRIS Optech 3D Scanner (OPTECH, 2008) from several positions with different lines of sight (Fig. 1) to get a preferably dense 3D point cloud. To keep the vegetation as a disturbing factor to a minimum only the last reflected impulse of the pulsed laser was recorded. The LiDAR point clouds were cleared of disturbing factors like vegetation and georeferenced in the PolyWorks software (INNOVMETRIC, 2011; OPPIKOFER *et alii*, 2012). In addition, to gain a better overview over the site and its prominent structures and to improve the field investigations (mapping and structural measurements) detailed Orthophotos as well as a DEM based on airborne laser scanning (ALS) with a resolution of 2 meters were used. The DEM suits very well as input data for differently exposed hillshades for a better understanding and identifying of the large morphological structures in the instability.

STRUCTURAL ANALYSES

The data collected in the field and the values gained by the Coltop3D analyses were stored and analysed with the software Dips6.0 (ROCSCIENCE, 2012) The orientations of the planes are displayed by its great circles and pole points in the Stereonet (lower hemisphere, equal area). Furthermore, kinematic tests for planar and wedge sliding as well as direct flexural toppling were performed to determine the possible failure modes.

In order to analyse the orientation of the discontinuity sets in the DEMs the Coltop3D software (TERRANUM, 2011) was applied (JABOYEDOFF *et alii*, 2007). The software computes surface normals out of the point cloud DEM and provides them with an orientation-specific colour. In the next step, by selecting surfaces with the same colour, Coltop3D was used to illustrates the orientations of the defined planes in a spherical projection (lower Stereonet) and to export the results as dip and dip direction in a text file (OPPIKOFER *et alii*, 2012).

For a better understanding of the possible movements within the rock, a comprehensive recording of persistance, spacing and roughness of the discontinuity sets according to WYLLIE & MAH (2004) was accomplished during the fieldwork.

DISPLACEMENT MEASUREMENTS

Displacements within the instability have been measured yearly by dGNSS surveys since 2008 (no measurement possible in 2012 because of bad weather conditions). Therefore three rover points were installed in the apparent instable parts of the mountain slope and one fixed point (Fig. 1) in a stable part above the main scarp, to receive a network of vectors which shows the point movement relative to each other. For this method, uncertainties in horizontal directions of 3-6 mm and in the vertical direction of 10-20 mm are assumed (HERMANNS et alii, 2011). Thus in this paper a movement is expected to be significant when it is larger than the uncertainty. Because of large height differences between the rover points and the fix point as well as annual systematic trends from un-modelled meteorological effects, the vertical uncertainty is much higher than the horizontal (BÖHME et alii, 2012) and hence must be interpreted carefully.

GEOELECTRIC

Three 2D resistivity profiles were measured in the valley bottom (Fig. 1) using the Lund system (DAHLIN, 1993) gradient electrode configuration and an ABEM SAS Terrameter 4000 (ABEM, 1999). Electrode separation was two meters (profile 1 and 2) and five meters (profile 3) giving a penetration depth of 25 and 60 meters respectively. This method has proven to be a powerful tool for mapping of drift deposits and fracture zones in bedrock (SOLBERG et alii, 2008; RØNNING et alii, 2009).
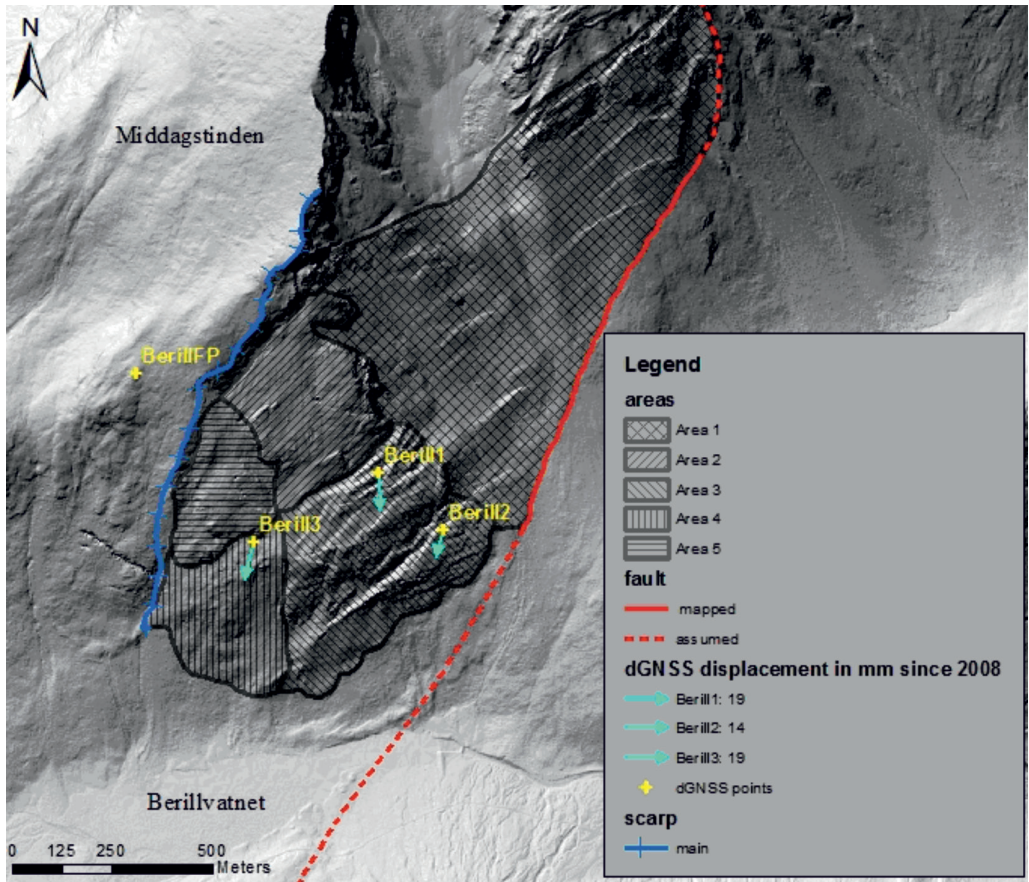

Fig. 2 - *Hillshade of the Berill instability with the different kinematic areas, morphological trace of the fault the main scarp and the relative movement of the dGNSS rover points*

267

RESULTS

MORPHOLOGY ON SLOPE

Based on the field mapping and ALS as well as Orthophoto analyses, four main areas (area 2-5) within the rock slope (Fig. 2) can be distinguished showing different types and/or amount of deformation. Similar deformation is suggested by counter scarps in surficial deposits E of the described rock slope and NW of the linear feature described as "Berill fault" (area 1).

EASTERN PART COVERED BY SURFICIAL DEPOSITS (AREA 1)

This area shows 3-4 meter deep depressions, which strike in the same direction as the counter scarps and the main scarp and deform the surficial deposits and limit towards the fault. Furthermore lateral moraines associated to younger Dryas glaciations can be found in this part of the slope instability. The fault strikes NNE-SSW and can be traced morphologically by a convex lineation along the slope which is 3-4 meters high and 1.5 km long but disappears in the valley.

UPPER MIDDLE PART (AREA 2)

Area 2 shows one coherent block with active rock fall at the lateral and frontal margins. Here large block fields have developed with up to several-meter- sized blocks.

LOWER MIDDLE PART (AREA 3)

Area 3 displays very prominent, up to 20 meter deep uphill facing scarps (counter scarps) with regular rock fall at the rockfaces. Hence the scarps are filled with meter sized blocks, so the real depth is masked. The distance between the individual rockfaces varies between 10 and 50 meters.

LOWER WESTERN PART (AREA 4)

Area 4 is characterised by large block fields with local repositioning structures. Where the blocks get smaller and mix with soil, surficial mass movements (e.g. shallow landslides) are present. Outcrops of the bedrock can only be found in some few parts and even then they are highly weathered and fractured. The transition to area 5 shows an accumulation of outcrops imbedded in large block fields.

UPPER WESTERN PART (AREA 5)

Area 5 shows one coherent block with defined lateral limits and many single, randomly distributed outcrops of the bedrock at the western and frontal margins that are surrounded by large blockfields. Since the major part of blocks in the deposits does not show repositioning structures (angular –partly very angular blocks) and there are highly fractured outcrops within the blockfields, the blocks are suggested to come from fragmentation on site but not by rock falls from above.

The horizontal displacements at the main scarp of the rock slope instability above area 2 and area 5 to the moving mass below is approximately 50 meters while the height of the scarp amounts to ~ 60 meters. The main scarp forms the back bounding limit both of area 2 and area 5.

STRUCTURAL ANALYSES

By analysing the structural data of the field and the DEMs, four main discontinuity sets have been identified (Tab. 1). The persistence, spacing and roughness descriptions refer to the classification of WYLLIE & MAH (2004).

FOLIATION (JS)

The foliation JS plunges with a mean dip/dip direction of 156/47 (field value) and varies over the whole area of the instable slope. In area 2 and area 5 the foliation forms distinct discontinuity surfaces with a high persistence, a close-moderate spacing and shows very little variability in the orientation. The surface of the foliation is here smooth and planar-undulating and both the main scarp and the frontal limit of area 2 are formed by the foliation. In the lower parts, especially in the counter scarps in area 2,the occurrence and the orientation are not constant. Here, the orientation of the foliation (dip direction) varies between NNE and SSW with

discontinuity set	DEM	Field data	spacing	persistence	roughness
J1	80/315±8	74/320±23	wide-very wide	high	rough,planar (undulating)
J2	81/048±14	78/45±20	wide-very wide	high	rough,planar (undulating)
JS	50/160±11	47/156±28	close-moderate	high	smooth, planar-undulated
JF		44/270±20	moderate-extremly wide	high	slickensided, planar
Lineation on JF groove marks on JS		31/245±11			
		42/138±16			

Tab. 1 - *Summary of the main discontinuity sets. The orientation data are presented as dip/dip direction with ± 1σ variability in degrees; the spacing, persistence and roughness descriptions refer to the classification of* WYLLIE *&*MAH *(2004)*

268

International Conference Vajont 1963-2013. Thoughts and analyses after 50 years since the catastrophic landslide   Padua, Italy - 8-10 October 2013

shallower inclinations between 5° and 40° with higher spacing and lower persistence values than in the upper area. This is because of folding in centimeter but also in meter scale with a fold axis towards the east.

JOINTS (J1, J2)

Two prominent joint sets are developed (J1, J2) that are both steep dipping with mean dip/dip direction values of 74/320 for J1 and 78/045 for J2 (field values). The spacing is wide – very wide, the persistence is high and the discontinuity surfaces are rough, planar, occasionally undulating. Most of the prominent structures like big fractures, cracks or lineaments visible in the field and on the DEM develop along these joint sets and single blocks or outcrops in the instability are limited by J1 and J2 or a combination of both. At the main scarp the occurrence of these joint sets is not as frequent as in the deforming parts and their persistence is much lower. This gets confirmed both by field observations and the analyses of the DEMs.

FAULT PLANE (JF)

The fault plane dips with a mean dip/dip direction of 44/270. The surface shows a quartz–feldspar remineralisation with lineation and frequent break offs that indicate normal fault movement. These lineaments do not occur continuously on the surface of the plane and the planes are partly undulated with varying orientations. Therefore the fault plane might follow a pre-existing discontinuity that was used as a preconditioned zone of weakness in the course of faulting. Because of its relative shallow orientation dipping into the mountain slope it can not be found in the DEMs, but the field investigation yield high, occasionally even very high persistence values. The spacing varies very much depending on the area. In some parts the outcrops of the surface recur in meter scale, in other parts it does not exist and in the lower parts (counter scarps) it plunges about 16° shallower than further up on the slope.

DISPLACEMENT MEASURMENTS

All rover points show a significant horizontal movement towards the south with a mean displacement rate of ~0.6 cm/year. The vertical movements over the last four years are not higher than the uncertainty and therefore are not discussed. The rover point Berill1 moves straight towards the south (176°) with a total displace-

ment of 19 mm since 2008, while Berill2 and Berill3 indicate a movement towards SSW (194° and 193°) with a displacement of 14 mm (Berill2) and 19 mm (Berill3) since 2008. Especially Berill1 and Berill2 show high variations in the east-west displacement, while Berill3 moves mainly constantly towards SSW (Fig. 3)

GEOELECTRIC

All resistivity profiles show low resistivity on the surface and higher resistivity at few meters depth. In addition, in all profiles there is one pronounced zone of low resistivity that separates areas of high resistivity that is ca. 10 m wide and dips either vertical or in the proposed dip direction of the fault. A second less pronounced zone of lower resistivity runs parallel to the former zones (Fig. 4).

DISCUSSION
GENESIS OF THE FAULT

The fault plane shows significant quartz-feldspar remineralisation with quartz/feldspar lineation that indicates that the fault was active in depth prior to exhumation to its present position. Moreover frequent break offs indicate a down-dip direction and hence a normal fault process (Fig. 5). The orientation of the lineation is parallel to the direction of the collapse of the Caledonian orogen. The low resistivity zone within the valley dips in the same direction and is thus interpreted to represent the prolongation of the fault in the valley. NGU opened trenches along the resistivity profiles that went
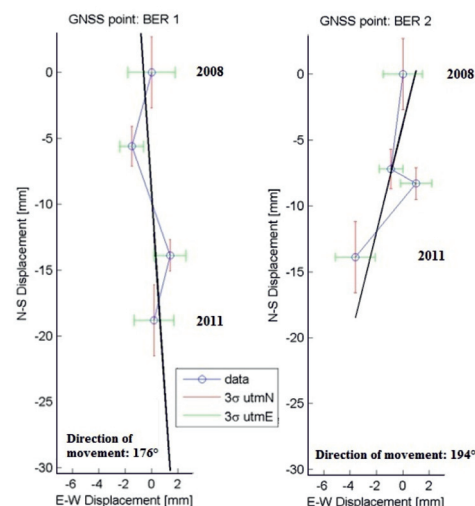

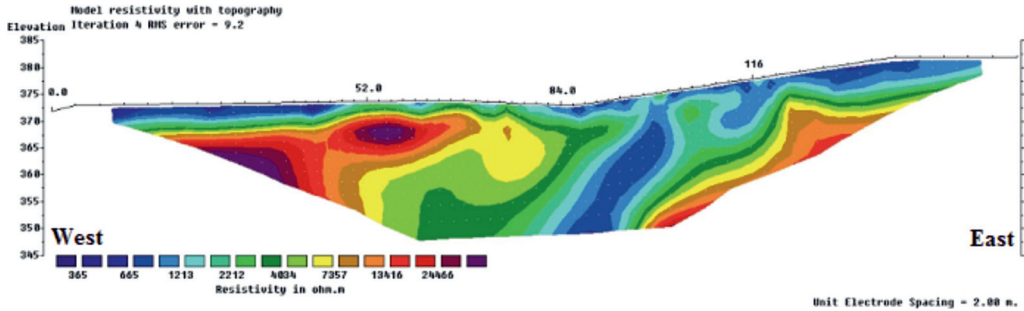Fig. 3 - Horizontal displacement rates of Berill 1 and Berill 2 since 2008

269

Fig. 4 - *Resistivity results along profile P1; low resistivity (blue colours) represent peat material at the surface and a 10 meter wide fractured zone in the bedrock dipping towards the west*

down into glacial deposits or down to the basement. No fault offsets or any soft sediment deformation features indicating seismic activity within the trenches were observed. Thus we interpret that the fault represents a fault active during the Caledonian collapse that has not been seismically reactivated in post glacial times.

INFLUENCE OF THE FAULT TO THE SLOPE DEFORMATION

The field data and the additional TLS data show, that the main scarp is mainly formed by the foliation JS which

Fig. 5 - *Pictures of the fault plane JF taken in the field a) lineation plunging 33/241; b) breakoffs on the hanging wall of the fault plane indicating a down dip direction*

plunges with a mean value of 52/154 (data taken in the field at the main scarp) and therefore does not daylight on the slope. However groove marks (Tab. 1) on the main scarp indicate a rockslide towards SSE. As the foliation is not daylighting, this movement becomes only possible because the foliation intersects with the fault plane forming an intersection lineament with the orientation 22/205 (Fig. 6). This orientation is 50° obliquely towards the orientation of the slope that strikes N 065° E with an average slope angle of 45°. The orientation of the sliding rock mass therefore moves out of the slope as a wedge failure with an angle of 50° relative to slope direction producing a positive offset along its SE boundary forming a step in the rilief similar to thrusting along the fault plane in an eastward direction (Fig. 5). Thus the Caledonian fault gets reactivated through the slope instability in form of an "apparent reverse fault". This direction is identical with the movement direction documented with the dGNSS rover stations Berill 1-3. Because the fault and the foliation are not present over the entire slope and their orientations are variable, also other deformation styles have developed on the slope in various sectors.
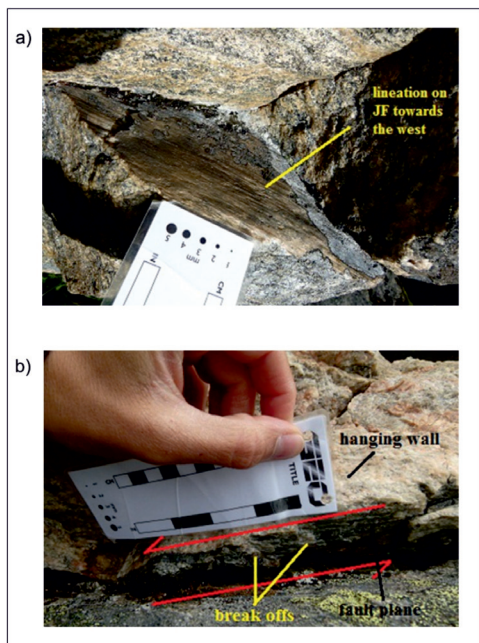
AREA 1

The bedrock of this area is covered by surficial glacial deposits and therefore it was neither possible to collect applicable structural data nor to install representative dGNSS points. But since area 1 also shows depressions, which strike in the same direction as the counter scarps in area 3, this part of the slope might follow a similar slope deformation process.

AREA 2

This coherent block has a surface area of 130.000 m² and is delimited by the joint set J1 in the front and

270

by J2 at its lateral limits. This block moves SSE along the foliation as shown by the groove marks at the back bounding scarp and therefore nearly in direction of the inclination of the slope. This movement builds up stress in the lower part of the slope in area 2.

AREA 3

dGNSS measurements and the kinematic analyses show, that area 2 is moving SSW that is therefore parallel to the intersection line of JS and JF (Fig. 6). However, as the foliation is less developed in this area deformation is also taken up by J1 by toppling towards SE (Fig. 7). This produces the counter scarps and might explain the varying east-west displacement rates of Berill1 and Berill2, which are installed at the top of the rock faces of the counter scarps. An SE direction of toppling and in combination with the SSW direction of wedge sliding on the intersection line of the foliation and the fault of this part of the instable slope results in the observed S movement of the dGNSS points. Area 2 and area 3 are described here as two different areas since the kinematic processes differ from each other, but still both areas outline one coherent block in the hillshade.

AREA 4

In area 4 no dGNNS point could be installed, because there are neither coherent blocks nor unfractured outcrops. The few existing outcrops are highly fractured with wide opened discontinuities likely related to high strain rates from the surrounding coherent blocks that "push" on this part of the slope.

AREA 5

The dGNSS measurements of the rover point Berill 3 and the Stereoplots indicate that the coherent block in the upper western part moves SSW and therefore differs from the moving direction of the upper eastern block. This block is separated from the block of area 2 along the joint set J2 and it moves parallel to intersection line of JS and JF towards SSW. The highly fractured outcrops of the bedrock at the western and frontal margins are assumed to be the result of varying movement directions of surrounding blocks.

CONCLUDING REMARKS

In conclusion after our thorough structural mapping in combination with dGNSS and geophysical
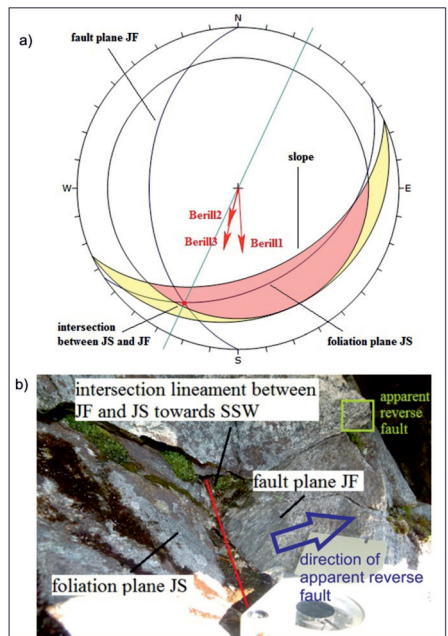

Fig. 6 - a) wedge sliding along the intersection line of the foliation JS and the fault JF; The input data are mean values of JF and JS taken in the lower parts (area 2) of the slope instability where the wedge developed; because of the slickensided surface of the fault and the smooth surface of the foliation the friction angle is estimated to be as low as 20°. The also plot shows the direction of the dGNSS rover points Berill1-3; b) field photo of the sliding on the intersection line between JF and JS with measured value of 21/201 (plunge/trend)
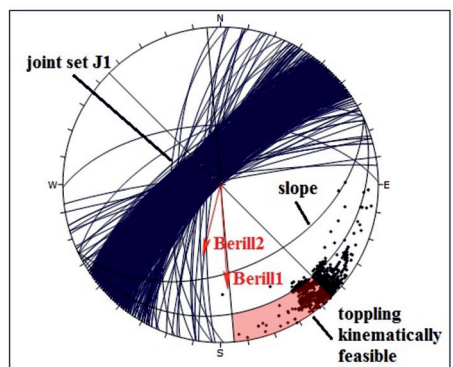

Fig. 7 - Toppling along the joint set J1 with the directions of the dGNSS rover points Berill1-2; the friction angle is with 25° higher than in Figure 3 because of a rougher discontinuity surface; the slope has a mean orientation of 45/155 (dip/dip direction)

investigations we summarize:
1. The fault plane is supposed to be a pre-existing

271

discontinuity which was exploited as a weakness zone in the course of faulting.

2. The quartz-feldspar remineralisation with lineation and break offs indicate a normal fault process towards the west.

3. Since the fault is parallel to the direction of the collapse of the Caledonian orogen and there was no evidence of fault deformation in the soft sediments in the trenches, we assume that the fault was active during the Caledonian collapse and was not reactivated in post glacial times.

4. The fault plane intersects with the foliation forming a wedge with an intersection lineament plunging SSW that takes part of the deformation. This direction coincides with dGNSS measurement of Berill3.

5. Due to different orientations of the slope and the wedge, the sliding rock mass produces a positive offset along its SE boundary and reactivates the fault plane locally in form of an ''apparent reverse fault''.

6. As the fault plane and the foliation plane do not occur constantly over the unstable slope, also other deformation styles developed on the slope, which are all terminated by the joint sets J1 and J2 and result in localized toppling towards the SE.

ACKNOWLEDGEMENTS

REFERENCES

ABEM (1999) - ABEM Terramter SAS 4000/SAS 1000. *Instruction Manual*. ABEM Printed Matter 93101.

ANDA E., BLIKRA L.H. & BRAATHEN A. (2002) - *The Berill Fault - first evidence of neotectonic faulting in southern Norway*. Norwegian Journal of Geology, **82**: 175-182.

BÖHME M., HERMANNS R.L., FISCHER L., OPPIKOFER T., BUNKHOLT H., DERRON M.H., CARREA D., JABOYEDOFF M. & EIKEN T. (2012) - *Detailed assessment of the deep-seated gravitational deformation at Stampa above Flåm, Norway*. In: EBERHARDT E., FROESE C., TURNER K. & LEROUEIL S. (EDS.). *Landslides and engineered slopes: protecting society through improved understanding*: 647-652. Taylor & Francis Group, Canada.

DAHLIN T. (1993) - *On the automation of 2D resistivity surveying for engineering and environmental applications,* Department of Engineering Geology, Lund Institutute of Technology. ISBN 91-628-1032-4. Lund Univesity.

GANERØD G.V. (2008) - *Structural mapping of the Åknes Rockslide, Møre and Romsdal County, Western Norway*. Geological Survey of Norway, Trondheim.

HACKER B.R., ANDERSEN T.B., JOHNSTON S., KYLANDER-CLARK A.R.C., PETERMAN E.M., WALSH E.O. & YOUNG D. (2010) - *High-temperature deformation during continental-margin subduction & exhumation: the ultrahigh-pressure Western Gneiss Region of Norway*. Tectonophysics **480** (1-4): 149-171.

HERMANNS R.L., BLIKRA L., ANDA, E., SAINTOT A., DAHLE H., OPPIKOFER T., FISCHER L., BUNKHOLT H., BÖHME M., DEHLS J., LAUKNES T., REDFIELD T., OSMUNDSEN P. & EIKEN T. (2011) - *Systematic mapping of large unstable rock slopes in Norway*. Proceedings of the Second World Landslide Forum, Rome.

HIPPOLYTE J-C., TARDY M., NICOUD G., BOURLES D., BRAUCHER R., MENARD, G. & SOUFACHE B. (2006) - *The resent fault scarps of the western Alps (France): Tectonic surface ruptures or gravitational sackung scarps? A combined mapping geomorphic, leveling and ^{10}Be-dating approach*. Tectonophysics, **418** (3-4): 255-276.

INNOVMETRIC (2011) - PolyWorks, p. 3D scanner and 3D digitizer software from InnovMetric Software.

JABOYEDOFF M., METZGER R., OPPIKOFER T., COUTURE R., DERRON M.-H., LOCAT J. & TURMEL D. (2007) - *New insight techniques to analyze rock-slope relief using DEM and 3D-imaging cloud points: COLTOP-3D software. Rock mechanics: Meeting Society's challenges and demands*. Proceedings of the 1st Canada - U.S. Rock Mechanics Symposium: 61-68. Taylor & Francis, Vancouver, Canada.

LI Z., BRUHN R.L., PAVLIS T.L., VORKING M. & ZENG Z. (2010) - *Origin of sackung uphill-facing scarps in the Saint Elias orogen, Alaska: LIDAR data visualization and stress modeling*. Geolocical Society of America Bulletin, **122**: 1585-1595

OPPIKOFER T., BUNKHOLT H.S.S., FISCHER L., SAINTOT A., HERMANNS R.L., CARREA D., LONGCHAMP C., DERRON M.-H., MICHOUD C. & JABOYEDOFF M. (2012) - *Investigation and monitoring of rock slope instabilities in Norway by terrestrial laser scanning*. In: EBERHARDT E., FROESE C., TURNER K. & LEROUEIL S. (EDS.). *Landslides and engineered slopes: protecting society through improved understanding*: 1235-1241. Taylor & Francis Group, Canada.

272

International Conference Vajont 1963-2013. Thoughts and analyses after 50 years since the catastrophic landslide   Padua, Italy - 8-10 October 2013

Optech (2008) - *ILRIS-3D. Intelligent Laser Ranging and Imaging System.*

Rocscience (2012) - *Dips 6.0. Graphical and Statistical Analysis of Orientation Data.*

Rønning J.S., Dalsegg E., Elvebakk H., Ganerød G.V. & Heincke B.H. (2009) - *Characterization of fracture zones in bedrock using 2D resistivity.* Proceedings from 5th Seminar on Strait Crossings, Trondheim: 439-444.

Solberg I.L., Rønning J.S., Dalsegg E., Hansen L., Rokoengen K. & Sandven R. (2008) - *Resistivity measurements as a tool for outlining quick clay extents and valley fill stratigraphy: feasability study from Buvika, Central Norway.* Canadian Geotechnical Journal, **45**: 210-225.

Terranum (2011) - *Coltop3D. LIDAR data processing and analyzing software for geologists.*

Thompson S.C., Clague J.J. & Evans S.G. (1997) - *Holocene activity of the Mt. Currie scarp, Coast Mountains, British Columbia, and implications for its origin.* Enviromental &Engineering Geosciences, **3** (3): 329-348.

Tveten E., Lutro O. & Thorsnes T. (1998) - *Geologisk kart over Norge, berggrunskart ÅLESUND, 1:250,000.* Geological Survey of Norway, Trondheim, Norway.

Wyllie D.C. & Mah C.W. (2004 eds.) - *Rock slope engineering: civil and mining.* 4th ed. Spon, London.